ChemPubSoc Europe

DOI: 10.1002/cplu.201402221

CHEMPLUSCHEM Full Papers

Thermoresponsive Polymer Nanoparticles Based on Viologen Cavitands

Elza D. Sultanova,[a] Ekaterina G. Krasnova,[b] Sergey V. Kharlamov,[b] Gulnaz R. Nasybullina,[b] Vitaly V. Yanilkin,[b] Irek R. Nizameev,[b] Marsil K. Kadirov,[b] Rezeda K. Mukhitova,[a] Lucia Y. Zakharova,[b] Albina Y. Ziganshina,*[a] and Alexander I. Konovalov[a]

In this study, the synthesis of new thermoactive polymer nanoparticles with a hollow and porous structure is reported. The nanoparticles consist of viologen cavitands linked with styrene bridges. The sizes of the nanoparticles and their pores are sensitive to temperature change. The temperature increase results in the swelling of the nanoparticles and in an increase in the permeability of the nanoparticle shell. The nanoparticles are characterized by the data of NMR, IR, and UV spectroscopies, and dynamic and static light scattering (DLS, SLS). The electrochemical behavior of the nanoparticles was investigated with cyclic voltammetry. The nanoparticles can be applied to the temperature-controlled binding and release of substrates as shown by the fluorescent dye rhodamine B. The nanoparticles encapsulate and release rhodamine B in response to the change in temperature from 25 to 40 °C.

Introduction

For many years the chemistry of nanomaterials maintained rapid progress, which resulted in the creation of a large number of complex polymer structures with interesting properties and functions.[1–4] Polymer nanoparticles,[5–9] the well-known representatives of this class of compounds, have found wide application in various areas, for example, as containers in drug-delivery systems;[11–13] markers in biological systems;[14] and building blocks for electronics[15] and optoelectronic devices.[16–18] Stimuli-responsive polymer nanoparticles are of particular interest to researchers because of their unique ability to change their structure, morphology, and properties[19–21] in response to an external stimulus (pH,[22] temperature,[23,24] solvent,[25] or light[26]). Fluorescence dyes are often applied as markers of their functional performance.[27–32]

Viologen-containing resorcinarene cavitands ($MVCA^{8+}$; Scheme 1) are redox-active macrocycles. They effectively bind multiply charged anions to form host–guest complexes by the four-centered electrostatic or donor–acceptor interaction of the viologen species with the charged or donor centers of anions.[33–35] The reversible reduction of the viologen groups to a radical cation or neutral form results in the weakening of host–guest complexes and to the appearance of new noncovalent interactions: intermolecular π dimerization of the viologen radical cations and the intermolecular hydrophobic interaction of resorcinarene platforms.[36,37] The bonding of $MVCA^{8+}$ in the nanoscale polymer matrix could open some opportunities for synthesizing new polyelectrolyte nanoparticles. A special feature of these nanoparticles is the electroswitchable change of the surface charge from a polycationic to a poly(cation radical) and neutral one, which leads to a considerable change in the

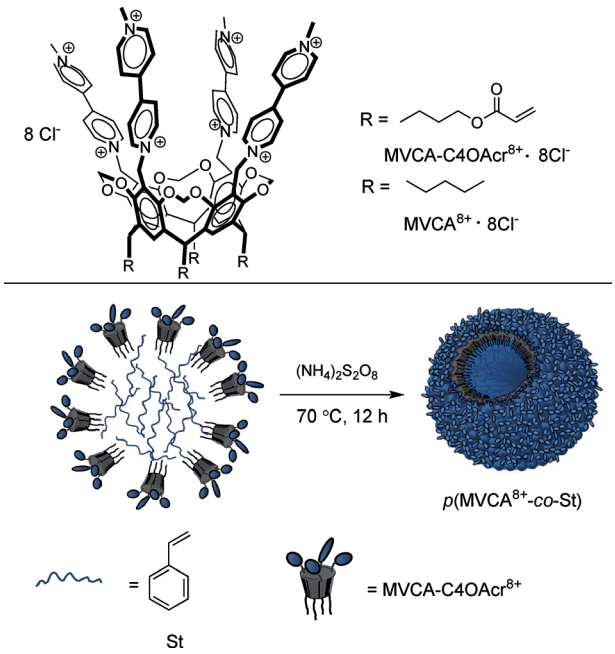

Scheme 1. Synthesis of $p(MVCA^{8+}$-*co*-St).

[a] E. D. Sultanova, R. K. Mukhitova, Dr. A. Y. Ziganshina, Prof. A. I. Konovalov
Department of Calixarene Chemistry
A.E. Arbuzov Institute of Organic and Physical Chemistry
Kazan Scientific Center, Russian Academy of Sciences
IOPC, Arbuzov str. 8, 420088 Kazan (Russia)
E-mail: az@iopc.ru

[b] E. G. Krasnova, Dr. S. V. Kharlamov, G. R. Nasybullina, Prof. V. V. Yanilkin, Dr. I. R. Nizameev, Prof. M. K. Kadirov, Prof. L. Y. Zakharova
A.E. Arbuzov Institute of Organic and Physical Chemistry
Kazan Scientific Center, Russian Academy of Sciences
IOPC, Arbuzov str. 8, 420088 Kazan (Russia)

Supporting information for this article is available on the WWW under http://dx.doi.org/10.1002/cplu.201402221.

structural, complexing, and material properties of the nanoparticles.

Herein, we report new polymer nanoparticles obtained by the polymerization of the viologen–resorcinarene cavitand (MVCA–C_4OAcr^{8+}·8Cl$^-$; Scheme 1) in the presence of styrene (St) as a comonomer. It was previously shown that MVCA^{8+} exhibits amphiphilic properties and self-assembles in aqueous media.[38] The hydrophobic tails of MVCA–C_4OAcr^{8+} are spaced by the resorcinarene cavity. This allows the creation of nanoparticles with pores formed by the linking of the remote side chains of the cavitand with the styrene bridges. In addition, the flexible alkyl chains form pores capable of "breathing", that is, of constricting/expanding. Such a nanoparticle structure holds great potential for binding/releasing systems, as it makes possible the reversible passage of substrates from the bulk solution into the particle cavity and back again.

Results and Discussion

The results obtained show that MVCA–C_4OAcr^{8+}·8Cl$^-$ (Table S1, Figures S1–S4 in the Supporting Information) is a good emulsifier of St in aqueous media. Mixing St (1–150 mM) with the aqueous solution of MVCA–C_4OAcr^{8+}·8Cl$^-$ (5 mM) and the ensuing ultrasonic treatment under an argon atmosphere leads to the formation of a clear 'oil-in-water' emulsion, which is stable for a long time (more than 20 days). Its polymerization for 12 h at 70 °C in the presence of the initiator $(NH_4)_2S_2O_8$ results in the formation of polymer particles (Scheme 1) that consist of MVCA^{8+} fragments linked with an St bridge.

The size and monodispersity of the particles depends on the ratio of MVCA–C_4OAcr^{8+} and St (Table S2, Figure S5). The best results were obtained for the 1:13 molar ratio (MVCA–C_4OAcr^{8+} and St respectively), at which the particles with a hydrodynamic diameter of about 140 nm (25 °C, polydispersity index (PDI) = 0.27) are formed. Hereafter, we study only the nanoparticles formed at a ratio of 1:13. The suspension of the nanoparticles was dialyzed for three days to remove the unreacted reagents and then lyophilized to form a powder. The powder was washed with acetone many times and dried to produce the *p*(MVCA^{8+}-*co*-St) nanoparticles. The elemental analysis shows that the ratio of MVCA–C_4OAcr^{8+} and St in the nanoparticles is approximately 1:2, that is to say, only approximately 15% of styrene is involved in the synthesis of *p*(MVCA^{8+}-*co*-St). The other 85% of St is only a part of the formation of the emulsions, but not in the polymerization of MVCA–C_4OAcr^{8+}. The excess amount of styrene was easily removed by the treatment of *p*(MVCA^{8+}-*co*-St) with acetone. The *p*(MVCA^{8+}-*co*-St) nanoparticles are highly soluble, stable, and do not stick together in water. Their molecular weight is in the range of (190 ± 20) kDa, as determined by static light scattering (Figure S6). The IR spectrum of *p*(MVCA^{8+}-*co*-St) shows the vibration signals of C=N bonds at 1637 cm^{-1}, the shift of the vibrational bands of C=O relative to the starting material owing to the polymerization of acrylate groups, and the overlay of the aromatic moieties of the cavitand and styrene at 3200–2800, 1450–1560, and 950–980 cm^{-1} (Figure S7).

According to the data obtained, the viologen groups are located on the surface of the nanoparticle, whereas the hydrophobic moieties are "hidden" inside the nanoparticles, in which a highly crowded environment should lead to a notable increase in the nuclear magnetization relaxation rates. Indeed, in the ^{13}C {^{1}H} NMR spectrum of *p*(MVCA^{8+}-*co*-St), only the signals of the viologen groups are observed. The signals of the hydrophobic part are dramatically broadened and were not detected (Figure 1). In the ^{1}H NMR spectrum of *p*(MVCA^{8+}-*co*-St), the signals of acrylic groups are not observed, whereas new broad signals related to the polymerized styrene appeared at δ = 7.3–7.8 and 1–2.5 ppm, thereby confirming the polymerization of *p*(MVCA^{8+}-*co*-St) with St (Figure S8). The ζ potential is + 23.5 mV (Figure S6), thereby confirming the location of viologen on the surface of the particles.

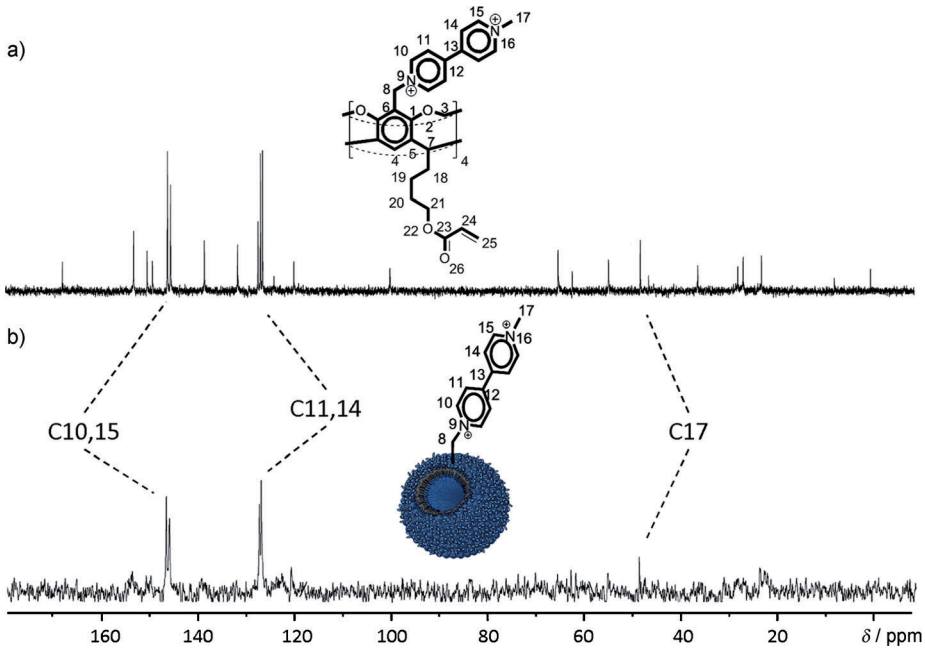

Figure 1. ^{13}C {^{1}H} NMR spectra of (a) MVCA–C_4OAcr^{8+}·8Cl$^-$ and (b) *p*(MVCA^{8+}-*co*-St) (600 MHz, D_2O, T = 303 K).

The nanoparticles *p*(MVCA^{8+}-*co*-St) are stable in water, do not coagulate, and aggregate because of the multicharged surface formed by the viologen groups. To define the mutual influence of viologens of *p*(MVCA^{8+}-*co*-St), an electrochemical experiment was carried out. Cyclic voltammograms of *p*(MVCA^{8+}-

co-St) are similar to those of viologen-cavitand MVCA–C_5^{8+} (Scheme S1).[39] The cyclic voltammogram shows a two-step reduction and reoxidation of the viologen groups of *p*(MVCA^{8+}-*co*-St) (Figure S9). The *p*(MVCA^{8+}-*co*-St) nanoparticles are reversibly reduced to the multi(cation radical) *p*(MVCA$^{4+\bullet}$-*co*-St) in the first step and the neutral nanoparticles *p*(MVCA^{0}-*co*-St) in the second step (Scheme S1). As is evident from the cyclic voltammetry curves (Figure S9), all the viologens of *p*(MVCA^{8+}-*co*-St) are reduced at the same potential, thus indicating the equivalence of their environment and the absence of their mutual influence. Such a reduction is possible if all the viologens of the cavitands and the cavitands themselves are spaced apart.[40] Clearly, water molecules and counterions separate the viologen groups, whereas flexible alkyl chains separate the *p*(MVCA^{8+}-*co*-St) cavitands.

The tails of the lower rim of MVCA^{8+} are separated by the cavitand frame, and their linking in the polymer nanoparticles results in the pore formation (Scheme 2). At the intramolecular linking of the neighboring tails of MVCA^{8+}, macrocycles that consist of 21 atoms or more (if the styrene groups are involved) are formed (Scheme 2). The intermolecular cross-linking of the two cavitands leads to the formation of pores that comprise 42 or more atoms. The bigger macrocyclic fragments of *p*(MVCA^{8+}-*co*-St) are generated by involving three, four, and more cavitands. Clearly, such large macrocyclic fragments that mainly comprise methylene groups have conformational mobility. They constrict and expand, which results in the "breathing" of the nanoparticles.

The constriction and expansion of *p*(MVCA^{8+}-*co*-St) was confirmed by DLS experiments. The hydrodynamic diameter of *p*(MVCA^{8+}-*co*-St) was measured in the temperature range of

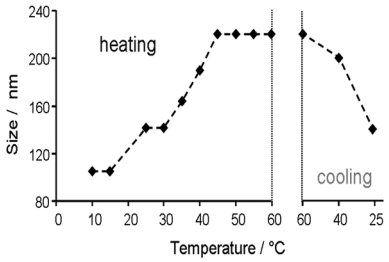

Figure 2. Temperature dependence of hydrodynamic diameter of *p*(MVCA^{8+}-*co*-St) (1.5 mg mL^{-1}, H_2O).

10–70 °C. According to the DLS data, the hydrodynamic diameter of the nanoparticles at 10 °C is about 100 nm, and it is almost two times larger at 40 °C (Figure 2, Table S3). Evidently, at high temperature the nanoparticle structure becomes more "loose", thereby allowing water to enter the cavity and expand its volume. Heating above 45 °C does not change the diameter of the nanoparticles, which almost reaches its maximum size. The reverse temperature decrease returns *p*(MVCA^{8+}-*co*-St) to its original size (Figure 2). According to the AFM data, the average size of *p*(MVCA^{8+}-*co*-St) in its dried state is about 65 nm (Figure S10). With increasing temperature, the polydispersity index of *p*(MVCA^{8+}-*co*-St) (Table S3) decreases, thereby confirming the swelling and not the coagulation of the particles.

The swelling of *p*(MVCA^{8+}-*co*-St) assumes that the nanoparticles have a hollow and porous structure. Carrying out the synthesis of the nanoparticles in an aqueous solution of rhodamine B (RhB), followed by the dialysis for three days at room temperature, results in the nanoparticles with the encapsulated dye (RhB@*p*(MVCA^{8+}-*co*-St)). In the UV/Vis spectrum of

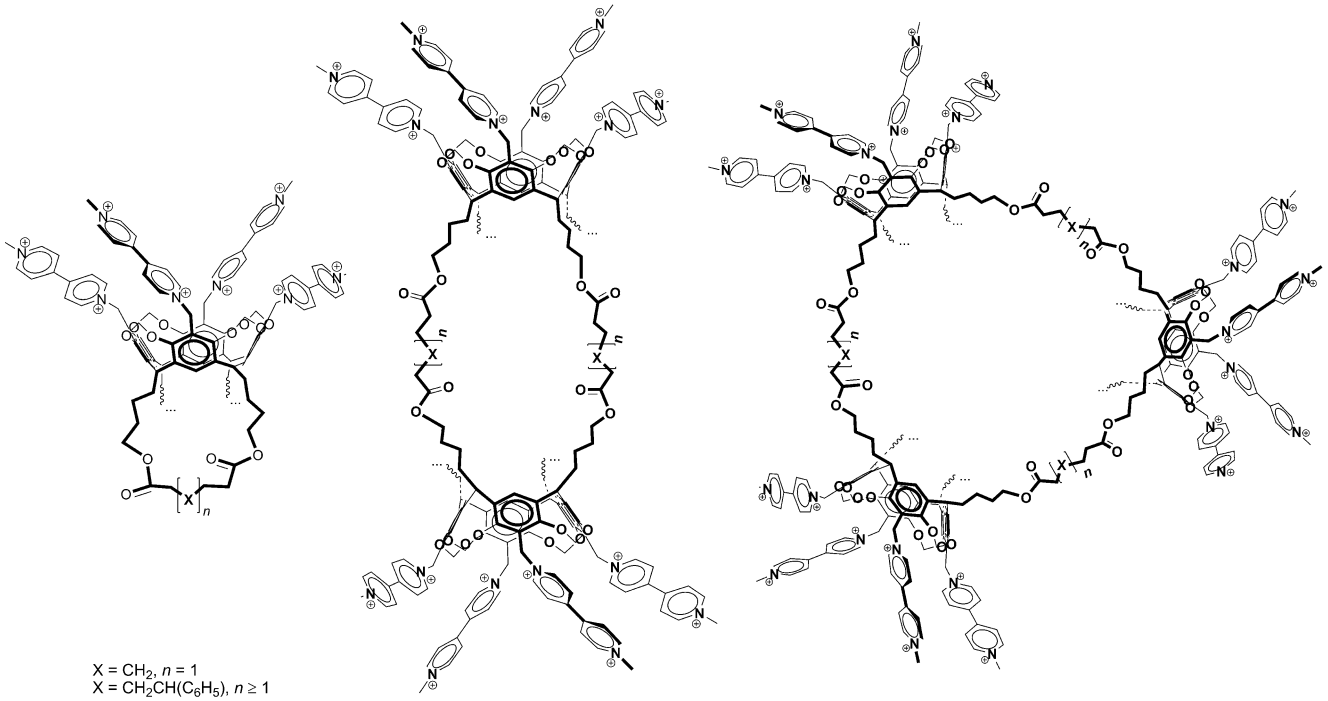

Scheme 2. Macrocyclic structures formed by intra- and intermolecular linking of MVCA–C_4OAcr^{8+}.

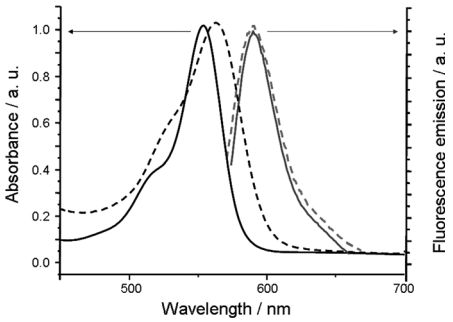

Figure 3. UV/Vis and fluorescence spectra of rhodamine B in aqueous media (solid lines) and encapsulated into *p*(MVCA^{8+}-*co*-St) (1 mg mL^{-1}) (dotted lines).

RhB@*p*(MVCA^{8+}-*co*-St) the absorption bands of the encapsulated dye are redshifted on account of the differences in the viscosity and polarity[41] of the nanoparticle cavity and the bulk solution (Figure 3). The fluorescence spectrum of the encapsulated rhodamine B is similar to the spectrum of the free dye with an emission band at 580 nm (Figure 3). The RhB@*p*(MVCA^{8+}-*co*-St) nanoparticles are quite stable: during their storage at room temperature for ten days, there was only a slight release of the dye molecules (≈7%) from the cavity *p*(MVCA^{8+}-*co*-St).

Reversible swelling and deswelling of *p*(MVCA^{8+}-*co*-St) assumes that the shell permeability of the nanoparticles is also sensitive to changes in temperature. The passing of a substrate from the bulk solution into the nanoparticle cavity and back is temperature-controlled (Scheme 3). The *p*(MVCA^{8+}-*co*-St) nanoparticles (1.5 mg mL^{-1}) were kept in aqueous solution of RhB (0.5 mg mL^{-1}) at room temperature and at 45 °C for 24 h. After dialysis for three days at room temperature, the solution incubated at 45 °C remained purple and the adsorption bands of RhB appeared in the UV/Vis spectrum, thereby confirming the encapsulation of the dye and the formation of RhB@*p*(MVCA^{8+}-*co*-St) (Figure 4). The entering of RhB into the nanoparticles has not been observed in the solution at room temperature (Figure 4). Importantly, the monomeric cavitand MVCA–C_5^{8+} does not interact with RhB at temperatures from 25 to 70 °C. The incubating of the solution of MVCA–C_5^{8+} with RhB at temperatures from 25 to 70 °C does not lead to the inclusion of RhB into the cavitand cavity: after dialysis for three days, the absorption bands of rhodamine B were not detected (Figure 4).

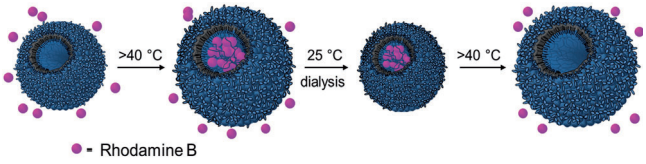

Scheme 3. Thermo-controlled encapsulation/release of rhodamine B in *p*(MVCA^{8+}-*co*-St).

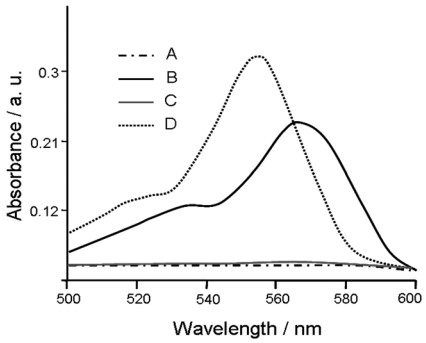

Figure 4. UV/Vis spectra of rhodamine B (starting concentration 1 mM) after incubation for 24 h in an aqueous solution of *p*(MVCA^{8+}-*co*-St) (1.5 mg mL^{-1}) at (A) 25 and (B) 45 °C followed by dialysis for three days; (C) after incubation for 24 h in an aqueous solution of MVCA–C_5^{8+} (1.5 mg mL^{-1}) at 70 °C followed by dialysis for three days; and (D) dialysate on the first day of the dialysis of the system rhodamine B (1 mM) + *p*(MVCA^{8+}-*co*-St) (1.5 mg mL^{-1}) at 45 °C.

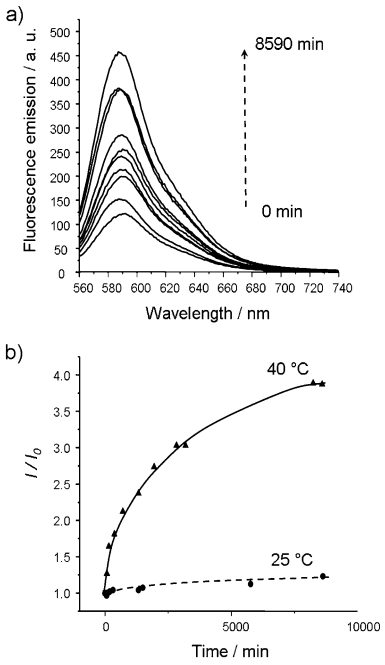

Figure 5. (a) Fluorescence spectra (25 °C) of RhB@p(MVCA^{8+}-*co*-St) (1 mg mL^{-1}) after heating at 40 °C for 0–8600 min. (b) Intensity change at 580 nm in fluorescence spectra of RhB@p(MVCA^{8+}-*co*-St) (1 mg mL^{-1}) after keeping the temperature at 25 and 40 °C (25 °C, H_2O).

The reheating of the RhB@*p*(MVCA^{8+}-*co*-St) solution leads to the release of rhodamine B from the nanoparticles. Upon heating, the size of the nanoparticles increases (Figure 5), the pores expand, and the dye molecules leave the cavity. The emission intensity of the dye increases as it passes into the bulk solution. As shown in Figure 5, the emission intensity in the fluorescence spectra of RhB@*p*(MVCA^{8+}-*co*-St) increases upon its heating at 40 °C, thus confirming the dye release. At room temperature, temporal changes in the emission spectrum are negligible. Thus, the nanoparticles obtained can indeed be used for the temperature-controlled binding and release of

substrates. A slight change in temperature from 25 to 40 °C causes significant changes in the nanoparticle size, thereby accelerating the release of substrates from the nanoparticle cavity.

Conclusion

In conclusion, we have obtained new thermoactive polymer nanoparticles *p*(MVCA^{8+}-*co*-St), which consist of viologen cavitands linked with polystyrene bridges. The nanoparticles are stable in aqueous media and their size changes in response to temperature. The temperature control of the swelling/deswelling of *p*(MVCA^{8+}-*co*-St) can be applied for the binding/release of the active reagents in the cavity of *p*(MVCA^{8+}-*co*-St). The redox-active surface of the nanoparticles can be reversibly recharged from polycation to poly(cation radical) and neutral forms. Nanoparticles with such properties could find applications in different areas of science: in drug-delivery systems or as a template for complex structure-building in material science. We intend to use them in the creation of redox-catalytic systems in which viologen cavitands would act as electron mediators.

Experimental Section

NMR spectroscopic experiments were carried out with an Avance 600 spectrometer (Bruker, Germany) equipped with a pulsed gradient unit capable of producing magnetic-field pulse gradients in the *z* direction of about 56 G cm^{-1}. D_2O was used as a solvent in all experiments. Chemical shifts were reported relative to HDO (δ = 4.7 ppm) as an internal standard. UV/Vis spectra were recorded with a Perkin–Elmer Lambda 25 UV/Vis spectrometer. Fluorescence emission spectra were recorded with a Cary Eclipse fluorescence spectrophotometer (USA). Rhodamine B was excited at 554 nm, and the fluorescence intensity was measured at 580 nm. The excitation and emission slit widths were 5 nm. A quartz cell of 1 cm path length was used for all fluorescence measurements. Imaging of the polymer nanoparticles was carried out by intermittent contact mode AFM with a MultiMode V scanning probe microscope (Veeco). A Zetasizer Nano instrument (Malvern, UK) equipped with a 4 mW He:Ne solid-state laser operating at 633 nm was used for SLS, DLS experiments, and ζ-potential measurements. Malvern dispersion technology software 5.0 was used for the analysis of particle size, ζ potential, and molecular weight. The cyclic voltammograms were recorded on a potentiostat P-30S under an inert atmosphere in H_2O/0.1 M NaCl media. The working electrode was a carbon glass disc electrode (*d* = 3.4 mm) pressed into Teflon. The electrode was cleaned by mechanical polishing before each measurement. Platinum wire was an auxiliary electrode. The potentials were measured relative to the saturated calomel electrode (SCE). The solutions were deaerated by bubbling argon in the solution. The temperature was 295 K. The diffusion nature of the peak currents i_p was proven by using the theoretical shape of the voltammogram and the linear dependence i_p–$v^{1/2}$; the adsorption nature was substantiated by the presence of an adsorption maximum and the linear dependence i_p–v by varying the potential scan rate from 10 to 200 mV s^{-1}.

Viologen-cavitand MVCA–C_4OAcr^{8+}·8Cl$^-$ was obtained from MVCA–C_4OH^{8+}·8Cl$^-$ as shown in Scheme 4. Cavitand MVCA–C_4OH^{8+}·8Cl$^-$ was synthesized similar to the method described in the literature[42] by using 3,4-dihydro-2*H*-pyran instead of 2,3-dihydrofuran in the condensation reaction with 2-methylresorcine.[43]

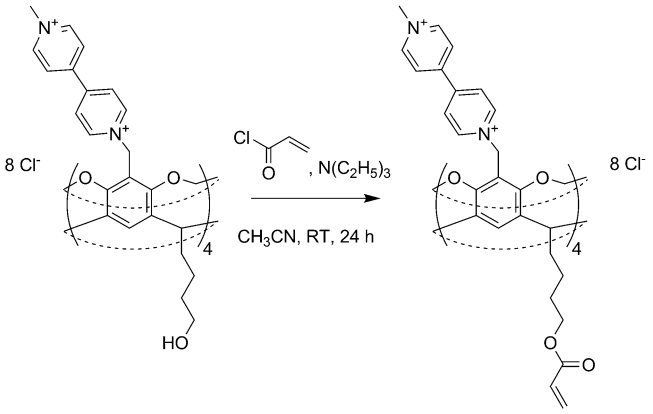

Scheme 4. Synthesis of MVCA–C_4OAcr^{8+}·8Cl$^-$.

Synthesis of MVCA–C_4OAcr^{8+}·8Cl$^-$

Triethylamine (0.3 mL, 2.17 mM) and acryl chloride (0.175 mL, 2.17 mM) were slowly added to a solution of MVCA–C_4OH^{8+}·8Cl$^-$ (0.2 g, 0.108 mM) in acetonitrile (10 mL) under an inert atmosphere. The mixture was kept at 25 °C for 24 h. The solid was filtered, washed with acetonitrile, and dialyzed in water for 3 h (6 mL versus 3×800 mL water). Water was removed under reduced pressure to obtain MVCA–C_4OAcr^{8+}·8Cl$^-$. Yield: 1.8 g, 81%; T_{decomp} > 210 °C; ^{1}H NMR (600 MHz, D_2O, 25 °C): δ = 1.37 (m, 8H), 1.71 (m, 8H), 2.41 (q, 8H), 4.08 (t, 8H), 4.49 (s, 12H), 4.74 (d, 4H), 4.80 (t, 4H), 5.74 (m, 4H), 5.834 (m, 4H), 5.86 (s, 8H), 6.02 (m, 4H), 6.42 (d, 4H), 7.68 (s, 4H), 8.48 (d, 8H), 8.53 (d, 8H), 9.04 (d, 8H), 9.16 ppm (d, 8H); ^{13}C NMR (D_2O, 25 °C): δ = 23.36, 27.17, 28.28, 36.58, 48.47, 55.04, 65.52, 100.34, 120.23, 124.36, 126.71, 127.18, 127.67, 131.88, 138.77, 145.77, 146.44, 149.51, 150.63, 153.44, 168.19 ppm; IR: $\tilde{\nu}$ = 1738, 1637 cm^{-1}; λ_{max} = 270 nm; elemental analysis calcd (%) for $C_{108}H_{112}N_8O_{16}$·8Cl·13H_2O: C 56.50, H 6.06, N 4.88, Cl 12.35; found: C 56.23, H 5.81, N 4.89, Cl 11.92. The NMR spectra and assignment of signals are shown in Table S1 and Figures S1–S4.

Synthesis of *p*(MVCA^{8+}-*co*-St)

Styrene (*c* = 65 mM, *V* = 0.118 mL) was added to a solution of MVCA–C_4OAcr^{8+}·8Cl$^-$ in water (*c* = 5 mM, *V* = 16.89 mL). The mixture was bubbled with argon for 30 min and then sonicated under an argon atmosphere until complete homogenization (approximately 80 min). The suspension was again bubbled with argon for 20 min and heated to 70 °C. Ammonium persulfate (0.2% of the mass of MVCA–C_4OAcr^{8+}·8Cl$^-$) was added, and the suspension was heated at 70 °C for 12 h. The final colloidal solution was dialyzed for 3 days (2 mL versus 3×800 mL water). Water was removed under reduced pressure. The solid formed was washed many times with acetone and dried. Yield: 0.16 g (59%); T_{decomp} > 230 °C. ^{1}H NMR (600 MHz, D_2O, 25 °C): δ = 4.48 (s, 12H), 5.85 (br s, 8H), 6.37 (br s, 4H), 8.49 (br m, 16H), 9.02 (br d, 8H), 9.11 ppm (br d, 8H); ^{13}C NMR (D_2O, 25 °C): δ = 48.47, 126.71, 146.44, 127.18, 15.77 ppm; IR: $\tilde{\nu}$ = 1716, 1637, 3200–2800, 1450–1560, 950–980 cm^{-1}; elemental analysis calcd (%) for $[(C_{108}H_{112}N_8O_{16})_{20}$·$(C_8H_8)_{40}$·$(Cl^-)_{22}$·$(SO_4^{2-})_{69}$·$(H_2O)_{400}]_n$: C 54.81, H 6.23, N 4.12, Cl 1.44, S 4.07; found: C 54.78, H 6.59, N 3.69, Cl 1.8, S 4.1.

Similar reactions with different concentration of styrene (0, 10, 35, and 150 mM) were carried out (Table S2 and Figure S5).

Synthesis of RhB@*p*(MVCA^{8+}-*co*-St)

Method A: RhB@*p*(MVCA^{8+}-*co*-St) was synthesized similarly to *p*(MVCA^{8+}-*co*-St) at 70 °C using an aqueous solution of rhodamine B ($c = 2.25$ mg mL^{-1} (5 mM)) instead of water. The final colloidal solution was dialyzed for 3 days (2 mL versus 3×800 mL water). Method B: A suspension that contained *p*(MVCA^{8+}-*co*-St) ($c = 2.5$ mg mL^{-1}) and rhodamine B ($c = 2.25$ mg mL^{-1}, (5 mM) was kept at 45 °C for 24 h. After that the solution was dialyzed for 3 days (2 mL versus 3×800 mL water).

Temperature-dependent swelling/deswelling of *p*(MVCA^{8+}-*co*-St)

An aqueous solution of *p*(MVCA^{8+}-*co*-St) ($c = 1.5$ mg mL^{-1}) was kept at a predetermined temperature (10–60 °C interval 5 °C) for 10 min and then the particle size was determined by DLS.

Release of rhodamine B from RhB@*p*(MVCA^{8+}-*co*-St)

A solution of RhB@*p*(MVCA^{8+}-*co*-St) ($C(p(\text{MVCA}^{8+}\text{-}co\text{-St})) = 1.5$ mg mL^{-1}) was kept at a predetermined temperature (25 and 40 °C). Aliquots of solution were taken at different times (0–4500 min) and fluorescence emission spectra were recorded.

Acknowledgements

This study was supported by the Russian Foundation for Basic Research (grant nos. 12-03-00379 and 14-03-00405).

Keywords: cavitands · nanoparticles · polymers · self-assembly · viologens

[1] G. Schmid, *Nanoparticles: From Theory to Applications*, Wiley-VCH, Weinheim, **2004**.
[2] J. P. Rao, K. E. Geckeler, *Prog. Polym. Sci.* **2011**, *36*, 887–913.
[3] J. Ramos, J. Forcada, R. Hidalgo-Alvarez, *Chem. Rev.* **2014**, *114*, 367–428.
[4] M. Elsabahy, K. L. Wooley, *Chem. Soc. Rev.* **2012**, *41*, 2545–2561.
[5] R. Fu, G. D. Fu, *Polym. Chem.* **2011**, *2*, 465–475.
[6] K. Landfester, *Angew. Chem. Int. Ed.* **2009**, *48*, 4488–4507; *Angew. Chem.* **2009**, *121*, 4556–4576.
[7] C. Pinto Reis, R. J. Neufeld, A. J. Ribeiro, F. Veiga, *Nanomedicine* **2006**, *2*, 8–21.
[8] K. Raemdonck, J. Demeester, S. D. Smedt, *Soft Matter* **2009**, *5*, 707–715.
[9] R. Ghosh Chaudhuri, S. Paria, *Chem. Rev.* **2012**, *112*, 2373–2433.
[10] F. Meng, Z. Zhong, J. Feijen, *Biomacromolecules* **2009**, *10*, 197–209.
[11] A. V. Kabanov, S. V. Vinogradov, *Angew. Chem. Int. Ed.* **2009**, *48*, 5418–5429; *Angew. Chem.* **2009**, *121*, 5524–5536.
[12] J. K. Oha, R. Drumright, D. J. Siegwart, K. Matyjaszewski, *Prog. Polym. Sci.* **2008**, *33*, 448–477.
[13] H. Wei, R. X. Zhuo, X. Z. Zhang, *Prog. Polym. Sci.* **2013**, *38*, 503–535.
[14] O. Lunov, T. Syrovets, C. Loos, J. Beil, M. Delacher, K. Tron, G. U. Nienhaus, A. Musyanovych, V. Mailänder, K. Landfester, Th. Simmet, *ACS Nano* **2011**, *5*, 1657–1669.
[15] H. I. Labouta, M. Schneider, *Int. J. Pharm.* **2010**, *395*, 236–242.
[16] W. Wu, S. Zhou, *Nano Rev.* **2010**, *1*, 5730.
[17] J. G. Park, J. D. Forster, E. R. Dufresne, *J. Am. Chem. Soc.* **2010**, *132*, 5960–5961.
[18] K. Li, B. Liu, *J. Mater. Chem.* **2012**, *22*, 1257–1264.
[19] C. Li, S. Liu, *Chem. Commun.* **2012**, *48*, 3262–3278.
[20] S. Xu, H. Lu, X. Zheng, L. Chen, *J. Mater. Chem. C* **2013**, *1*, 4406–4422.
[21] C. L. Liu, C. H. Lin, C. C. Kuo, S. T. Lin, W. C. Chen, *Prog. Polym. Sci.* **2011**, *36*, 603–637.
[22] R. Dong, B. Zhu, Y. Zhou, D. Yan, X. Zhu, *Angew. Chem. Int. Ed.* **2012**, *51*, 11633–11637; *Angew. Chem.* **2012**, *124*, 11801–11805.
[23] C. Pietsch, U. S. Schubert, R. Hoogenboom, *Chem. Commun.* **2011**, *47*, 8750–8765.
[24] X. Wang, O. S. Wolfbeis, R. J. Meier, *Chem. Soc. Rev.* **2013**, *42*, 7834–7869.
[25] E. Kim, J. Lee, D. Kim, K. E. Lee, S. S. Han, N. Lim, J. Kang, C. G. Park, K. Kim, *Chem. Commun.* **2009**, 1472–1474.
[26] H. Jin, Y. Zheng, Y. Liu, H. Cheng, Y. Zhou, D. Yan, *Angew. Chem. Int. Ed.* **2011**, *50*, 10352–10356; *Angew. Chem.* **2011**, *123*, 10536–10540.
[27] P. N. Ezhilarasi, P. Karthik, N. Chhanwal, C. Anandharamakrishnan, *Food Bioprocess Technol.* **2013**, *6*, 628–647.
[28] A. Kowalczuk, R. Trzcinska, B. Trzebicka, A. H. E. Müller, A. Dworak, C. B. Tsvetanov, *Prog. Polym. Sci.* **2014**, *39*, 43–86.
[29] K. K. Cotí, M. E. Belowich, M. Liong, M. W. Ambrogio, Y. A. Lau, H. A. Khatib, J. I. Zink, N. M. Khashab, J. F. Stoddart, *Nanoscale* **2009**, *1*, 16–39.
[30] L. Graña Suárez, W. Verboom, J. Husken, *Chem. Commun.* **2014**, *50*, 7280–7282.
[31] S. Theisinger, K. Schoeller, B. Osborn, M. Sarkar, K. Landfester, *Macromol. Chem. Phys.* **2009**, *210*, 411–420.
[32] H. Dong, V. Mantha, K. Matyjaszewski, *Chem. Mater.* **2009**, *21*, 3965–3972.
[33] A. Y. Ziganshina, S. V. Kharlamov, E. Kh. Kazakova, Sh. K. Latypov, A. I. Konovalov, *Mendeleev Commun.* **2007**, *17*, 145–147.
[34] G. R. Nasybullina, V. V. Yanilkin, N. V. Nastapova, D. E. Korshin, A. Y. Ziganshina, A. I. Konovalov, *J. Inclusion Phenom. Macrocyclic Chem.* **2012**, *72*, 299–308.
[35] V. V. Yanilkin, G. R. Nasybullina, A. Y. Ziganshina, I. R. Nizamiev, M. K. Kadirov, D. E. Korshin, A. I. Konovalov, *Mendeleev Commun.* **2014**, *24*, 108–110.
[36] G. R. Nasybullina, V. V. Yanilkin, A. Y. Ziganshina, V. I. Morozov, E. D. Sultanova, D. E. Korshin, V. A. Milyukov, R. P. Shekurov, A. I. Konovalov, *Russ. J. Electrochem.* **2014**, *50*, 756–772.
[37] G. R. Nasybullina, V. V. Yanilkin, A. Y. Ziganshina, V. I. Morozov, E. D. Sultanova, D. E. Korshin, Yu. S. Spiridonova, A. S. Balueva, A. A. Karasik, A. I. Konovalov, *Russ. Chem. Bull.* **2013**, *62*, 2158–2170.
[38] V. V. Yanilkin, G. R. Nasybullina, N. V. Nastapova, A. Y. Ziganshina, D. E. Korshin, Y. S. Spiridonova, M. Gruner, W. D. Habicher, A. A. Karasikand, A. I. Konovalov, *Electrochim. Acta* **2013**, *111*, 466–473.
[39] G. R. Nasybullina, V. V. Yanilkin, N. V. Nastapova, A. Y. Ziganshina, D. E. Korshin, Yu. S. Spiridonova, A. A. Karasik, A. I. Konovalov, *Russ. Chem. Bull.* **2012**, *61*, 2295–2310.
[40] J. H. Mondal, S. Ahmed, D. Das, *Langmuir* **2014**, *30*, 8290.
[41] D. A. Hinckley, P. G. Seybold, D. P. Borris, *Spectrochim. Acta* **1986**, *42*, 747–754.
[42] X. Leaym, S. Kraft, S. H. Bossmann, *Synthesis* **2008**, *6*, 932–942.
[43] B. C. Gibb, R. G. Chapman, J. C. Sherman, *J. Org. Chem.* **1996**, *61*, 1505–1509.

Received: July 11, 2014
Revised: September 17, 2014
Published online on October 14, 2014